Medial Axis Approximation of River Networks for Catchment Area Delineation

Farid Karimipour, Mehran Ghandehari and Hugo Ledoux

Abstract The hydrological catchment areas are commonly extracted from digital elevation models (DEMs). The shortcoming is that computations for large areas are very time consuming and even may be impractical. Furthermore, the DEM may be inaccessible or in a poor quality. This chapter presents an algorithm to approximate the medial axis of river networks, which leads to catchment area delineation. We propose a modification to a Voronoi-based algorithm for medial axis extraction through labeling the sample points in order to automatically avoid appearing extraneous branches in the media axis. The proposed approach is used in a case study and the results are compared with a DEM-based method. The results illustrate that our method is stable, easy to implement and robust, even in the presence of significant noises and perturbations, and guarantees one polygon per catchment.

Keywords Voronoi diagram · Delaunay triangulation · Medial axis · River network · Catchment area delineation

1 Introduction

A catchment area is a hydrological unit where precipitations that fall into this area, eventually end up in the same river. The raster-based algorithms, which usually use DEM in their approach, are very common in automated catchment area

F. Karimipour (✉) · M. Ghandehari
Department of Surveying and Geomatics Engineering, College of Engineering, University of Tehran, Tehran, Iran
e-mail: fkarimipr@ut.ac.ir

M. Ghandehari
e-mail: ghandehary@ut.ac.ir

H. Ledoux
OTB, Section GIS Technology, Delft University of Technology, Delft, The Netherlands
e-mail: h.ledoux@tudelft.nl

A. Abdul Rahman et al. (eds.), *Developments in Multidimensional Spatial Data Models*, Lecture Notes in Geoinformation and Cartography,
DOI: 10.1007/978-3-642-36379-5_1,

delineation (Martz and Garbrecht 1992, 1993; Turcotte et al. 2001; Chorowicz et al. 1992; Mark 1984; Tarboton 1997; Lin et al. 2006; Yang et al. 2010; Nelson et al. 1994; Mower 1994; Jones et al. 1990). Nevertheless, they have some difficulties: Firstly, the raster-based analyses can be time consuming. Secondly, the accuracy of these methods depends on the quality and type of the DEM used, that is, *per se*, affected by the accuracy, density and distribution of the source data, the smoothness of the terrain surface and the deployed interpolation method (Li et al. 2005). Thirdly, the limitations in flow direction computation affect the results. The flow path is biased to the grid axes and the water is trapped in sinks and flat areas. Finally, the raster to vector conversion of boundaries may create some intersections and the boundaries are not explicitly defined.

On top of these, the river network may be the only available data in some cases, and the DEM is either inaccessible or in a poor quality. In this situation, the best approximation of the catchment areas would be to extract the region that is closer to a certain river segment than to any other and consider it as the catchment area corresponding to that river (Gold and Dakowicz 2005; Dillabaugh 2002; McAllister 1999). This approximation is achieved through medial axis (MA) extraction, which is defined as the set of points that are equidistant from at least two points on the boundary of the shape.

This chapter aims to verify the hypothesis stated by Gold and Snoeyink (Gold and Snoeyink 2001) to use a Voronoi-based MA extraction method (called one-step crust and skeleton algorithm) for delineation of catchment areas: The river network is sampled with a set of points, and Delaunay triangulation and Voronoi diagrams are used to extract the MA, which results in an approximation of the catchment areas. The initial investigation shows that this method gives a fair approximation of the catchments. However, there are many extraneous branches in the extracted MA (the catchment area, here) due to small perturbations of the sample points.

This chapter proposes a modification to the one-step crust and skeleton algorithm to overcome the above issue through labeling the sample points. Each river segment is considered as a curve segment and its corresponding sample points are assigned the same label. Furthermore, we explain how the catchment polygons are constructed from the extracted MA, which is a set of lines. The conceptual structure and the results illustrate that our method is stable, easy to implement and robust, even in the presence of significant noise and perturbations and guarantees one polygon per catchment.

The rest of the chapter is organized as follows: Sect. 2 represents some geometric definitions, including Delaunay triangulation, Voronoi diagram, medial axis and two definitions related to sampling. Section 3 describes the one-step crust and skeleton algorithm. Simplification and pruning methods for filtering the MA are introduced briefly in Sect. 4. In Sect. 5, we propose a method for catchment area delineation through a modification to the algorithm presented in Sect. 3. The proposed method is used in a case study in Sect. 6 and the results are compared with a DEM-based method. Finally, Sect. 7 discusses the concluding remarks.

2 Geometric Definition

This section represents some geometric preliminaries, including Delaunay triangulation, Voronoi diagram and medial axis. Two definitions related to sampling are presented. In this section, $\mathcal{O}$ is a 2D object, $\partial\mathcal{O}$ is its boundary and S $\subset \partial\mathcal{O}$ is a dense sampling of $\partial\mathcal{O}$.

2.1 Delaunay Triangulation

Definition 1 Given a point set S in the plane, the *Delaunay triangulation* (DT) is a unique triangulation (if the points are in general position) of the points in S that satisfies the circum-circle property: the circum-circle of each triangle does not contain any other point $s \in S$ (Ledoux 2006) (Fig. 1a).

2.2 Voronoi Diagram

Definition 2 Let S be a set of points in R^2. The Voronoi cell of a point $p \in S$, denoted as $V_p\ (S)$, is the set of points $x \in R^2$ that are closer to p than to any other point in S:

$$V_p(S) = \left\{x \in R^2 | \|x - p\| \leq \|x - q\|, q \in S, q \neq p\right\} \tag{1}$$

The union of the Voronoi cells of all points $s \in S$ forms the *Voronoi diagram* of S, denoted as $VD(S)$:

$$VD(S) = \bigcup V_p(S), p \in S \tag{2}$$

Figure 1b shows the Voronoi diagrams of a set of points in the plane. Delaunay triangulation and Voronoi diagram are dual structures: the centers of circum-circles of the Delaunay triangles are the Voronoi vertices; and joining the adjacent

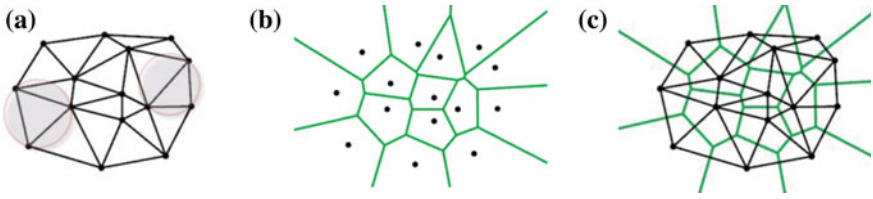

Fig. 1 **a** Delaunay triangulation and **b** Voronoi diagram of a set of points in the plane; and **c** their duality

generator points in the Voronoi diagram yields their Delaunay triangulation (Fig. 1c) (Karimipour et al. 2010).

For Voronoi diagram of sample points S, the Voronoi vertices are classified into *inner* and *outer vertices*, which lie inside and outside $\mathcal{O}$, respectively. Then, the Voronoi edges are classified into three groups: edges between two inner vertices (*inner Voronoi edges*), edges between two outer vertices (*outer Voronoi edges*), and edges between an inner and an outer vertices (*mixed Voronoi edges*).

2.3 Medial Axis

The medial axis was first introduced by Blum (1967) as a tool in image analysis. Grassfire model is the most popular definition of the MA with an intuitive concept: consider starting a fire on the boundary of a shape in the plane. The fire starts at the same moment, everywhere on the boundary and it propagates with homogeneous velocity in every directions. The MA is the set of points where the front of the fire collides with itself, or other fire front. Mathematically:

Definition 3 The *medial axis* is (the closure of) the set of points in $\mathcal{O}$ that have at least two closest points on the object's boundary $\partial\mathcal{O}$. (Amenta et al. 1998).

Another description defines the medial axis as the centers of the set of maximal disks contained in $\mathcal{O}$ (a maximal disk is a disk contained in a shape that is not completely covered by another disk contained in the shape) (Fig. 2).

2.4 Local Feature Size and r-Sampling

Quality of the sample points S has a direct effect on the extracted MA. *Local feature size* is a quantitative measure to determine the level of details at a point on a curve, and the sampling density needed for curve reconstruction and MA extraction.

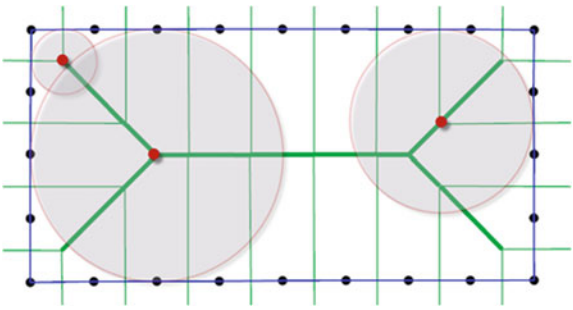

Fig. 2 The MA of a 2D curve (*rectangle*)

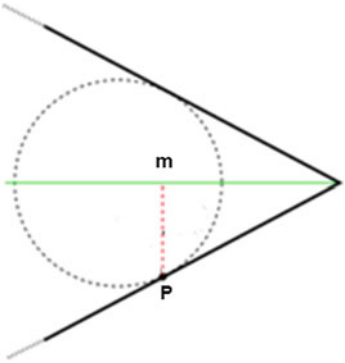

Fig. 3 The local feature size of a point p (*line segment pm*) (Wenger 2003)

Definition 4 The *local feature size* of a point $p \in \partial\mathcal{O}$, denoted as $LFS(p)$, is the distance from p to the nearest point m on the MA (Amenta et al. 1998) (Fig. 3).

Definition 5 The object $\mathcal{O}$ is *r-sampled* by a set of sample points S if for each point $p \in \partial\mathcal{O}$, there is at least one sample point $s \in S$ that $\| p\text{-}s \| \leq r \divideontimes LFS(p)$ (Amenta et al. 1998).

The value of r is less than 1; and usually $r = 0.4$ is considered a reasonably dense sampling (Amenta et al. 1998). Figure 4 shows an example where sample points around the center are denser in order to provide a proper sampling.

3 One-Step Crust and Skeleton Algorithm

Amenta et al. (1998) proposed a Voronoi-based algorithm (called crust algorithm) to reconstruct the boundary from a set of sample points forming the boundary of a shape. Gold and Snoeyink (2001) improved this algorithm so that both the boundary (crust) and the MA (skeleton) are extracted, simultaneously and the coined the name "one-step crust and skeleton" for this algorithm.

In the one-step crust and skeleton algorithm every Voronoi/Delaunay edge is either part of the crust (Delaunay) or the skeleton (Voronoi), which can be determined by a simple *inCircle* test. Each Delaunay edge (D_1D_2 in Fig. 5a) belongs to two triangles ($D_1D_2D_3$ and $D_1D_2D_4$ in Fig. 5a). For each Delaunay edge, there is a dual Voronoi edge (V_1V_2 in Fig. 5a).

Suppose two triangles $D_1D_2D_3$ and $D_1D_2D_4$ have a common edge D_1D_2 whose dual Voronoi edge is V_1V_2. The $InCircle(D_1, D_2, V_1, V_2)$ determines the position of V_2 respect to the circle passes through D_1, D_2 and V_1. If V_2 is outside the circle, D_1D_2 belongs to the crust (Fig. 5b). If V_2 is inside, however, V_1V_2 belongs to the skeleton (Fig. 5c).

As illustrated in Fig. 6, if the one-step crust and skeleton algorithm is applied on a river network, the extracted MA yields a fair approximation of the

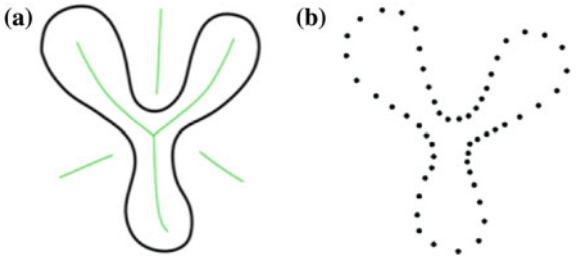

Fig. 4 **a** A curve with its MA (*green curves*); **b** An *r*-sampling of the curve (Wenger 2003)

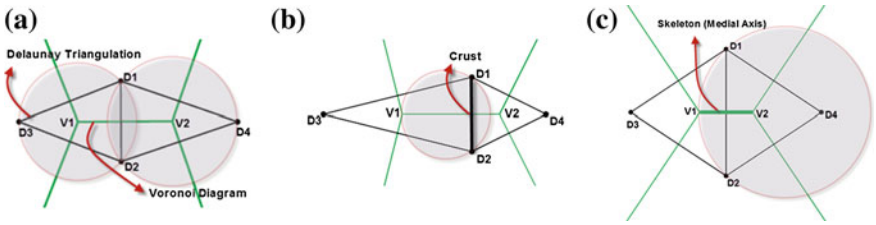

Fig. 5 One-step crust and skeleton extraction algorithm: **a** Delaunay triangulation and Voronoi diagram of four sample points D_1 to D_4; **b** V_2 is outside the circle passes through D_1, D_2 and V_1, so D_1D_2 belongs to the crust; **c** V_2 is inside the circle passes through D_1, D_2 and V_1, so V_1V_2 belongs to the skeleton

Fig. 6 MA extraction of a river network, which yields an approximation of the catchments

corresponding catchments. However, there are many extraneous branches in the extracted MA due to small perturbations of the sample points, which must be filtered out as discussed in the next section.

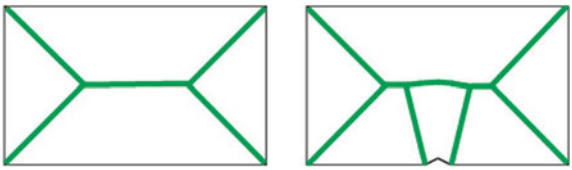

Fig. 7 Similar shapes may have significantly different MAs in the presence of boundary perturbations

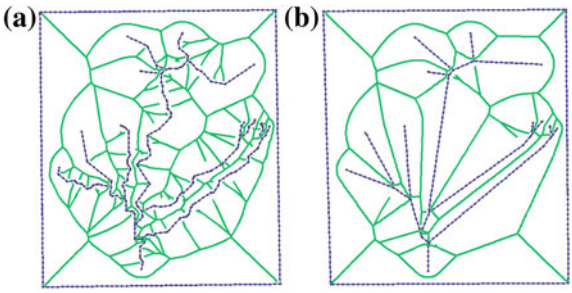

Fig. 8 MA approximation of a river network: **a** before and **b** after simplification

4 Filtering the Extraneous Edges in the Medial Axis

The MA is inherently unstable under small perturbations; i.e., it is very sensitive to the small changes of the boundary, which produce many extraneous branches in the MA. As a result, two similar shapes may have significantly different MAs (Fig. 7). Filtering extraneous branches is a common approach to extract the major parts of the MA. Such filtering may be applied as pre-processing through simplifying (smoothing) the boundary, or as post-processing through pruning that eliminate the extraneous branches of the extracted MA.

4.1 Simplification

Some of the filtering methods simplify the boundary before computing the MA by removing perturbations or boundary noises (Siddiqi et al. 2002; Attali and Montanvert 1996) (Fig. 8). Although these methods aim to remove unwanted boundary noises, they may not provide the ideal results: (1) Some extraneous edges may still exist in the extracted MA; (2) the distinction between boundary data and noise can be difficult; and (3) these methods can alter the topological structure and thus the MA position.

4.2 Pruning

The purpose of the pruning algorithms, as a post-processing step, is to remove extraneous branches of the extracted MA, in order to preserve only the stable parts

of the MA. An importance value (based on angle, distance, area, etc.) is assigned to each branch, and then the branches with the importance value less than a given threshold are removed (Attali et al. 1995; Chazal and Lieutier 2005; Attali and Montanvert 1994; Giesen et al. 2009).

The pruning algorithms have some drawbacks: (1) Some extraneous branches may not be eliminated; (2) Eliminating extraneous branches usually shorten the main branches; (3) A disconnection in the main structure of the MA may occur; (4) Most of the pruning methods do not preserve the topology of complex shapes; (5) In some cases, multiple parameters are required and it is difficult to determine appropriate thresholds, simultaneously. Finally, most pruning methods require user checks at the end.

5 Proposed Algorithm for Medial Axis Extraction

In this section, we propose an improvement to the one-step crust and skeleton algorithm through labeling the sample points in order to automatically avoid appearing extraneous branches in the MA, and show how our proposed approach improves the results (Karimipour and Ghandehari 2012; Ghandehari and Karimipour 2012).

Figure 9a illustrates the MA of a shape extracted using the one-step crust and skeleton algorithm. As this figure shows, this algorithm detects some extraneous edges as parts of the MA, which are filtered through simplification or pruning. We observed that such extraneous edges are the Voronoi edges created between the sample points that lie on the same segment of the curve. It led us to the idea of labeling the sample points in order to automatically avoid appearing such edges in the MA (Fig 9b).

We consider the shape boundary as different curve segments ∂_i such that:

$$\partial O = \bigcup_{i=1}^{n} \partial O_i \tag{3}$$

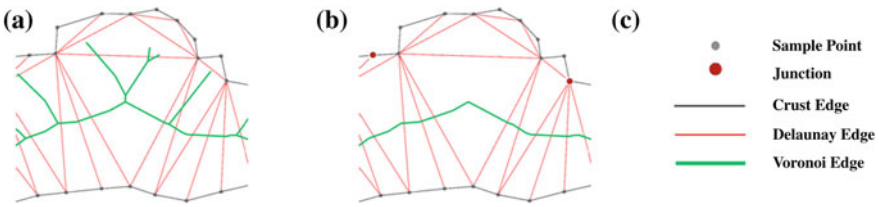

Fig. 9 **a** One-step crust and skeleton algorithm detects some extraneous edges as parts of the MA. They are the Voronoi edges created between the sample points that lie on the same segment of the curve; **b** our proposed method automatically avoid such edges in the MA

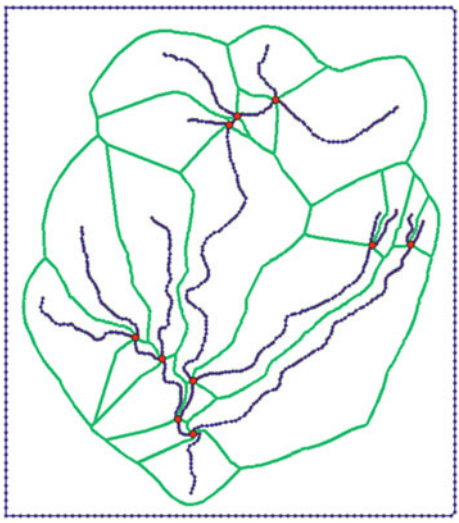

Fig. 10 MA approximation of river network using our proposed algorithm avoids appearing the extraneous branches in the MA

Inner and outer Voronoi edges do not intersect with ∂, but mixed Voronoi edges do (Giesen et al. 2007). The same applied to the Delaunay edges: Delaunay edges of the sample points S are classified into three classes: *Mixed Delaunay edges* that join two consecutive points and belong to the crust; and *inner/outer Delaunay edges* that join two non-consecutive points and are completely inside/outside $\mathcal{O}$ (all Delaunay vertices lie on the $\partial\mathcal{O}$). Note that the inner/outer/mixed Voronoi edges are dual to the inner/outer/mixed Delaunay edges.

Based on the above definitions, the extraneous MA edges are the inner Voronoi edges whose both end points lie on the same curve segment. However, the dual of the main MA edges are the inner Voronoi edges (or its dual inner Delaunay edges) whose end points lie on two different curve segment. Therefore, the main idea of the proposed approach is to remove all the MA edges whose corresponding Delaunay vertices lie on the same boundary curve.

We start with labeling the sample points: Each segment of the shape is assigned a unique label; and all of its sample points are assigned the same label. The points that are common between two curve segments are called *junctions*, which are assigned a unique negative label to distinguish them from other sample points.

Filtering in our proposed method is not a pre- or post-processing step, but it is performed simultaneously with the MA extraction. To extract the MA, we use one-step crust and skeleton algorithm. Each Delaunay edge passes the *InCircle* test: If the determinant is negative and the corresponding Delaunay vertices have the same labels or one of them is a junction, that Delaunay edge is part of the crust. Otherwise, if the determinant is positive and the corresponding Delaunay vertices have different labels, its dual is added to the MA. Figure 10 illustrates the result of using our proposed algorithm to extract the MA of the river network presented in Fig. 6, in which the extraneous branches are automatically avoided.

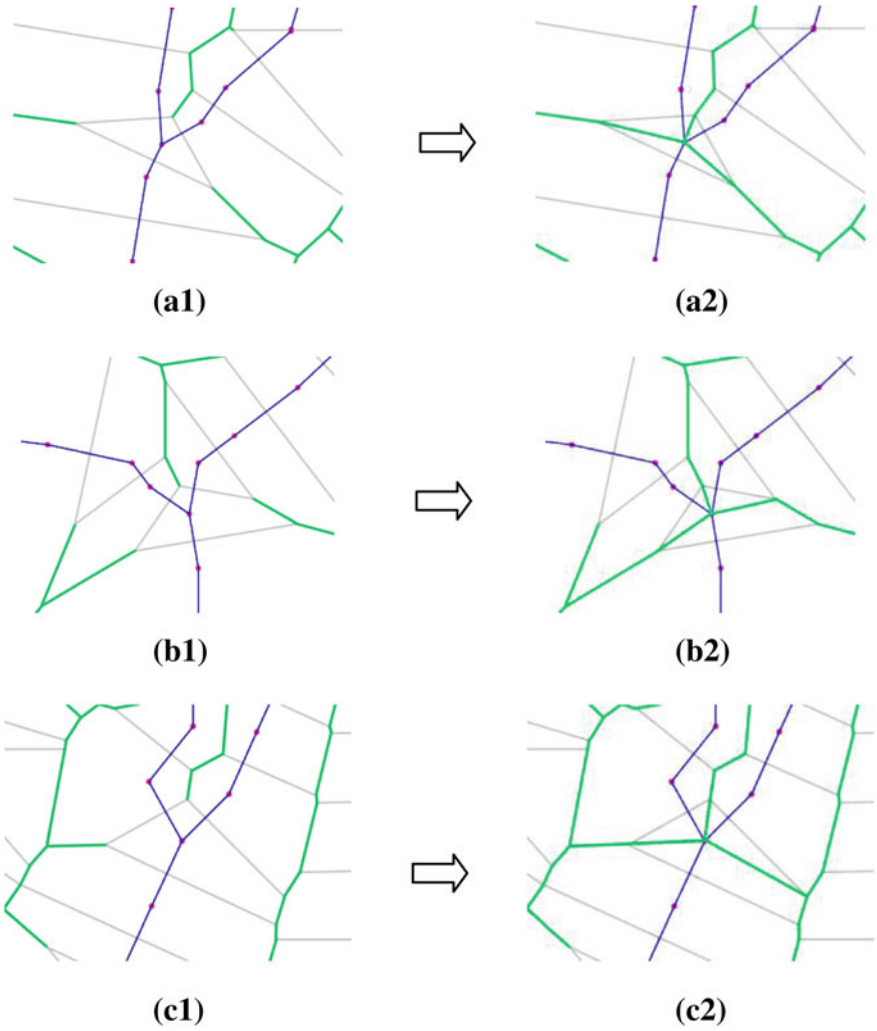

Fig. 11 Different configuration of the MA around the junction

5.1 Closing the Polygons

The calculated MA is a set of lines, whose union does not necessarily construct real polygons (catchments, here). A final check is needed to find and fix the gaps. For this, each junction is connected to three of the vertices of the Voronoi cell that contains the junction. Depending on the configuration of the MA around the junction, three cases may happen:

- The Voronoi cell of the junction point is a triangle (Fig. 11a1). Here, the three vertices of the Voronoi cell are connected to the junction point (Fig. 11a2).

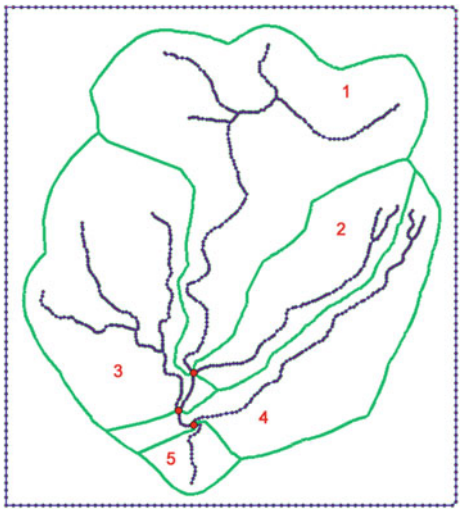

Fig. 12 Hierarchical delineation of catchments using the MA

- The Voronoi cell of the junction point has more than three vertices, and k of these vertices are dangle nodes. If $k = 3$ (Fig. 11b1), the three dangle vertices are connected to the junction point (Fig. 11b2). Otherwise, if $k < 3$ (Fig. 11c1), the k dangle nodes plus 3-k random vertices are connected to the junction (Fig. 11c2).

5.2 Hierarchical Delineation

Having extracted the MA using the one-step crust and skeleton algorithm, each branch of the streams is assigned a catchment polygon. Merging the polygons extracted for the branches of the same stream yields the catchment area of that stream. In our proposed method, however, a single polygon is already assigned to all the branches of the stream because they all have the same label (Fig. 12).

6 Implementation Results

We used the proposed approach for a case study and compared the result with a DEM-based method. Numerous techniques exist for automated extraction of catchment boundaries from DEM. The DEM is as a set of points in a Triangular Irregular Network (TIN) (Nelson et al. 1994; Jones et al. 1990), or a raster surface (Mower 1994). These methods usually simulate rainfall and assume that water always flows along the path of steepest descent.

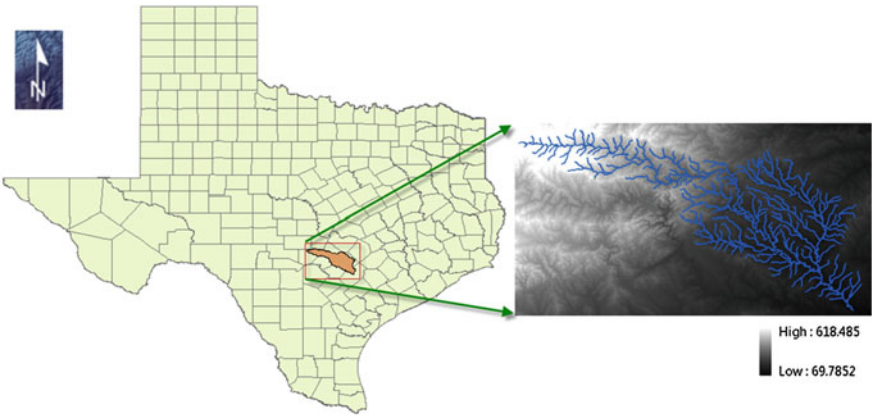

Fig. 13 Study area located at the upstream of San Marcos River in the south of Texas

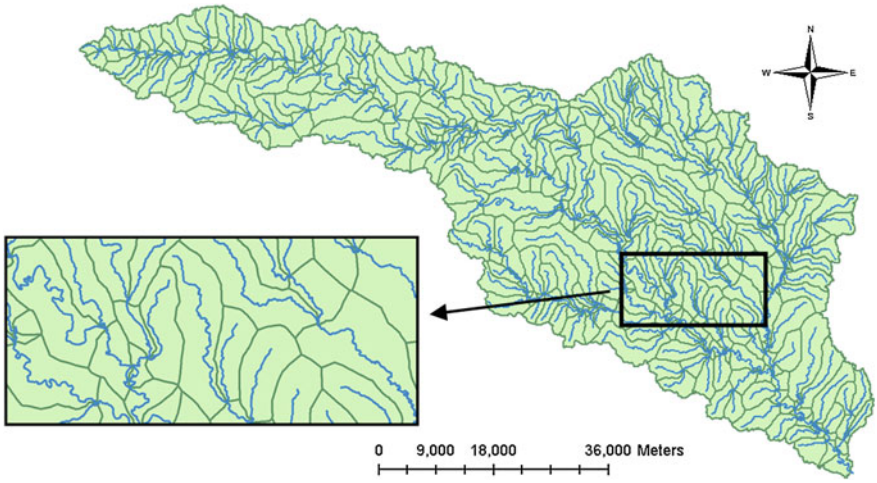

Fig. 14 Catchment area delineation of the study area from the river network using the proposed method

The study area is San Marcos basin located at the upstream of San Marcos River in the south of Texas State, USA (Fig. 13). It has an area of 3528 km^2 and its elevation varies from 70 to 618 m. The data used here consists of river data from the National Hydrography Dataset (NHD) and a raster DEM of the San Marcos Basin from the National Elevation Dataset (NED) with the spatial resolutions of 1 arc-second (approximately 30 m). Figures 14 and 15 respectively illustrate the catchment area delineated using the proposed approach and the DEM-based method implemented in ArcHydro extension of ArcGIS software, which are fairly similar.

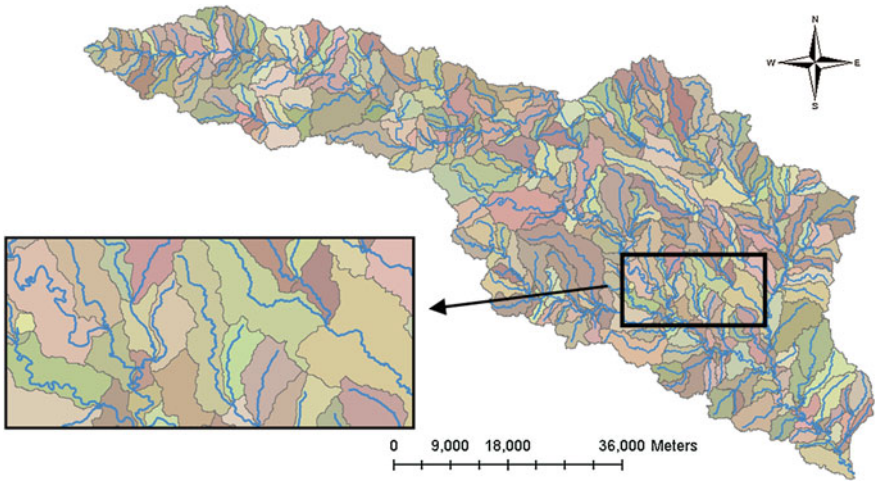

Fig. 15 Catchment area delineation of the study area from DEM using ArcHydro

7 Conclusion and Future Works

This chapter verifies the idea of Gold and Snoeyink (Gold and Snoeyink 2001) to use the MA of river networks as an approximation of the catchment areas. The advantages are: (1) It is simple and easy to implement (2) The method can handle very large areas and produce catchment polygons quickly. While, by increasing the spatial resolution of DEM or for a large area, the size of the raster DEMs required to delineate catchments would be large and the related processing like flow direction and flow accumulation can be so time consuming.

We also modify the algorithm proposed by Gold and Snoeyink to automatically avoid appearing extraneous branches in the MA. This solution is simple, easy to implement and robust to boundary perturbations of the sample points (river network).

The proposed method gives an approximation of the catchment area boundaries using the MA of the river networks. Although the output of the proposed method may not be as accurate as DEM-based methods, it can be efficiently used when DEM data is either inaccessible or in a poor quality.

References

Martz LW, Garbrecht J (1993) Automated extraction of drainage network and watershed data from digital elevation models. JAWRA 29:901–908

Turcotte R, Fortin JP, Rousseau A, Massicotte S, Villeneuve JP (2001) Determination of the drainage structure of a watershed using a digital elevation model and a digital river and lake network. J Hydrol 240:225–242

Chorowicz J, Ichoku C, Riazanoff S, Kim YJ, Cervelle B (1992) A combined algorithm for automated drainage network extraction. Water Resour Res 28:1293–1302

Martz LW, Garbrecht J (1992) Numerical definition of drainage network and subcatchment areas from digital elevation models. Comput Geosci 18:747–761

Mark DM (1984) Part 4: mathematical, algorithmic and data structure issues: automated detection of drainage networks from digital elevation models. cartographica. Int J Geogr Info Geovisualization 21:168–178

Tarboton DG (1997) A new method for the determination of flow directions and upslope areas in grid digital elevation models. Water Resour Res 33:309–319

Lin WT, Chou WC, Lin CY, Huang PH, Tsai JS (2006) Automated suitable drainage network extraction from digital elevation models in Taiwan's upstream watersheds. Hydrol Process 20:289–306

Yang W, Hou K, Yu F, Liu Z, Sun T (2010) A novel algorithm with heuristic information for extracting drainage networks from Raster DEMs. Hydrol Earth Syst Sci Discuss 7:441–459

Nelson EJ et al (1994) Algorithm for precise drainage-basin delineation. J Hydraul Eng 120:298

Mower JE (1994) Data-parallel procedures for drainage basin analysis. Comput Geosci 20:1365–1378

Jones NL, Wright SG et al (1990) Watershed delineation with triangle-based terrain models. J Hydraul Eng 116:1232

Li Z, Zhu Q, Gold C (2005) Digital terrain modeling: principles and methodology. CRC Press, USA

Gold C, Dakowicz M (2005) The crust and skeleton–applications in GIS. Second international symposium on Voronoi diagrams in science and engineering, pp 33–42

Dillabaugh C (2002) Drainage basin delineation from vector drainage networks. Joint international symposium on geospatial theory, processing and applications, Ottawa, Ontario, Canada

McAllister M (1999) The computational geometry of hydrology data in geographic information system. PhD thesis, University of British Columbia

Gold C, Snoeyink J (2001) A one-step crust and skeleton extraction algorithm. Algorithmica 30:144–163

Ledoux H (2006) Modelling three-dimensional fields in geo-science with the Voronoi diagram and its dual. PhD Thesis. School of Computing, University of Glamorgan, Pontypridd, Wales, UK

Karimipour F, Delavar MR, Frank AU (2010) A simplex-based approach to implement dimension independent spatial analyses. Comput Geosci 36:1123–1134

Blum H et al (1967) A transformation for extracting new descriptors of shape. Models for the perception of speech and visual form 19, 362–380

Amenta N, Bern MW, Eppstein D (1998) The crust and the beta-skeleton: combinatorial curve reconstruction. Graphical Models Image Process 60:125–135

Wenger R (2003) Shape and medial axis approximation from samples. PhD thesis. The Ohio State University

Siddiqi K, Bouix S, Tannenbaum A, Zucker SW (2002) Hamilton-Jacobi Skeletons. Int J Comput Vision 48:215–231

Attali D, Montanvert A (1996) Modeling noise for a better simplification of skeletons. In: IEEE international conference on image processing, vol 3. pp 13–16

Attali D, di Baja G, Thiel E (1995) Pruning discrete and semicontinuous skeletons. In: Proceedings of the 8th international conference on image analysis and processing, vol 974. pp 488–493

Chazal F, Lieutier A (2005) The Lambda Medial Axis. Graph Models 67:304–331

Attali D, Montanvert A (1994) Semicontinuous skeletons of 2D and 3D shapes. In: Proceedings of the second international workshop on visual form, pp 32–41

Giesen J, Miklos B, Pauly M, Wormser C (2009) The scale axis transform. In: Proceedings of the 25th annual symposium on computational geometry, pp 106–115

Karimipour F, Ghandehari M (2012) A stable Voronoi-based algorithm for medial axis extraction through labeling sample points. In: Proceedings of the 9th international symposium on Voronoi diagrams in science and engineering (ISVD 2012), New Jersey, USA

Ghandehari M, Karimipour F (2012) Voronoi-based curve reconstruction: issues and solutions. The international conference on computational science and its applications (ICCSA 2012), Lecture notes in computer science (LNCS), vol 7334. pp 194–207. Springer, Brazil

Giesen J, Miklos B, Pauly M (2007) Medial axis approximation of planar shapes from union of balls: a simpler and more robust algorithm. In: Proceedings of the 19th Canadian conference on computational geometry (CCCG), pp 105–108